Anal. Bioanal. Electrochem., Vol. 9, No. 5, 2017, 630-639

Analytical & Bioanalytical Electrochemistry

2017 by CEE
www.abechem.com

Full Paper

In-Situ Synthesis of $LiFePO_4$/Carbon Cauliflower-Like by Hydrothermal Reaction for Using in Lithium Ion Batteries

Mina Rezaeipayam,[1,2] Mehran Javanbakht,[1,2,*] Hossein Ghafarian-Zahmatkesh,[1,2] Ehsan Golestani[1,2] and Mehdi Ghaemi[2,3]

[1]*Department of Chemistry, Amirkabir University of Technology, Tehran, Iran*
[2]*Renewable Energy Research Center, Amirkabir University of Technology, Tehran, Iran*
[3]*Department of Chemistry, Science Faculty, Golestan University, Gorgan, Iran*

*Corresponding Author, Tel.: +98 21 64545806
E-Mail: mehranjavanbakht@gmail.com

Received: 1 May 2017 / Accepted: 15 May 2017 / Published online: 15 August 2017

Abstract- The active cauliflower-like LiFePO4 (LFP/Cin) material was synthesized with hydrothermal process in the presence of glucose and then calcined at 600 °C. The physical properties, particle size and morphology of obtained samples were investigated with the X-ray diffraction (XRD), Scanning Electron Microscope (SEM) and Transmission Electron Microscope (TEM). The electrochemical performance of nano-composites was studied by cyclic voltammetry (CV), electrochemical impedance spectroscopy (EIS) and galvanostatic cycling performance. The CV curves show that LFP/C_{in} has higher electrochemical reactivity for lithium insertion and extraction than the LFP conventional cathode material. EIS measurements demonstrated that R_{ct} for LFP/C_{in} is 70 and 50 percent lower compared to LFP and LFP/C_{ex} respectively. The initial discharge capacity of $LiFePO_4/C_{in}$ cathode material delivers about 133.92 mAh g^{-1} (82% of theoretical capacity) at 0.1 C and cycling stability with 96.3% of capacity retention after 40 cycles at 0.1 C. Electrochemical tests demonstrate that in-situ carbon coating play an important role in the improvement of battery performance with increasing the conductivity, reduce the particles size and unique structure.

Keywords- Lithium iron phosphate, Cauliflower-like morphology, Cathode material, Lithium ion batteries, Glucose, $LiFePO_4$/C

1. INTRODUCTION

Lithium-ion batteries (LIBs), as an important, clean and rechargeable electrical energy source and green applications, with high energy density and power capability are extensively used as electrical power sources in portable electronics devices, such as mobile telephones,

laptop computers, video-cameras and even though in hybrid electric and electric vehicles (HEVs and EVs). Therefore, batteries with high capacities, cycling stability and good rate performance are in high demand in current society [1-3]. The first report of $LiFePO_4$ by the Goodenough in 1997 has generated worldwide attention into the olivine structure [4], because of the high theoretical capacity of 170 mAh g^{-1}, flat discharge voltage about 3.45 V (*vs.* Li/Li^+), low cost and toxicity, environmental benignity, and high safety. However, the main downsides of olivine LFP are its intrinsically low electronic conductivity ($\sim 10^{-9}$ $S.cm^{-1}$ at room temperature) and low ionic conductivity [5-8]. To solve these inherent drawbacks, two ways have been adopted. First, coating a conductive thin layer of carbon or another conductive material onto the surfaces of LFP particles [8-13] or doping with transition metals [14,15] and second, synthesize of nano particles and decreasing the Li-ion transport distance [16,17]. Recently, tremendous efforts have been conducted by several research groups for increasing the electronic and ionic conductivity with carbon coating using various methods such as, hydrothermal, sol-gel, solid state and so on. One of the best methods for synthesis of electrode active materials is hydrothermal method due to its advantages such as economic, homogeneous and narrow size distribution, high crystallinity and morphology [18,19]. Gao et al [20] prepared LFP/C composite using solid-state reaction, which exhibited an initial discharge capacity of 145 mAh g^{-1} and exhibits excellent electrochemical performances but the size of particles were about 1 micrometer. M. Rastgoo et al had two-stage heating during hydrothermal process to synthesize LFP microcrystals, which exhibited a capacity of about 118 mAh g^{-1} and electronic conductivity. However, the low capacity resulting from microcrystals, limits the practical applications [21].

Recently we have studied improvement of electrochemical properties of some developed flower like LFP [21], rhombohedral LFP [22], LFP/graphene nanocomposite [23], bow-tie-like lithium iron phosphate nanocrystals [24] and CuO/graphene Nano sheets modified LFP [25] by hydrothermal method. In the present work, to enhance the conductivity and improve electrochemical performance of lithium iron phosphate (LFP), glucose was utilized as an additive for active material. We successfully synthesized LFP with a thin layer of electron conductor carbon coating by a hydrothermal method. The effect of added glucose on the structural characteristics, morphology and electrochemical performance of the composites electrode were also investigated and presented. When the obtained powders were used as cathode materials in LIBs, the LFP/C_{in} nanoparticles showed the best electrochemical performances among other electrodes.

2. EXPERIMENTAL SECTION

2.1. Materials preparation

All chemicals were purchased from Merck CO, Ltd Germany (in analytical grade). The LFP powders have been synthesized via a hydrothermal reaction from the starting materials $LiOH.H_2O$, $FeSO_4.7H_2O$, and $NH_4H_2PO_4$ without any purification. The initial concentrations of Li, Fe and P in the solution were set in the 3:1:1 molar ratio, respectively. In a typical synthesis firstly, 10 mmol $NH_4H_2PO_2$, 30 mmol $LiOH\text{-}H_2O$ and 10% w/w glucose (as a carbon source and the oxidation inhibitor only for LFP/C_{in}) were dissolved in double distilled water and then $FeSO_4.7H_2O$ aqueous solution (10 mmol) was added gradually to the first mixture under stirring. A mixture of glycerol and distilled water (50:50) was used as solvent for both samples LFP/C_{in} and LFP/C_{ex}. Each of the prepared mixture was then transferred to a Teflon vessel and the total solvents volume has been brought to 150 ml.

The vessel was bubbled by N_2 to emit O_2 from reaction media and sealed in a stainless-steel autoclave and then it was immersed in a silicon oil bath that was previously heated on the hotplate magnetic stirrer. The hydrothermal treatment was performed for 6 h under constant stirring (500 rpm) at 180 °C. After cooling it to room temperature, the light green precipitates were gathered by centrifuging and dried in vacuum oven at 60 °C for 12 h. For LFP/C_{ex} 10% w/w of glucose was added to obtained samples for carbon source before the calcined step. The obtained powders (LFP, LFP/$C_{ex,}$ and LFP/C_{in}) were calcined at 670 °C for 6 h under flowing N_2 atmosphere.

2.2. Characterization of materials

The composition, crystallinities and phase purity of the prepared samples were recorded using powder X-ray diffraction (XRD) Equinox 3000 with Cu Kα radiation (λ=0.15418 nm). The ZEISS transmission electron microscope (TEM) SIGMA 900 was operated at an Accelerating voltage of 80 kV. Field-emission scanning electron microscopy (FE-SEM) measurement was carried out by ZEISS SIGMA.

2.3. Electrochemical measurement

Electrochemical tests were carried out using Li metal and cathode active material (LFP, LFP/C_{ex} and LFP/C_{in}) as electrodes, 1 M $LiClO_4$ in propylene carbonate as electrolyte and micro-pores polypropylene membrane (Celgard 2400) as separator. The composite electrode for electrochemical measurements was prepared by mixing the as-prepared active material powders, ultra-pure graphite powder as conductor and poly (vinylidene fluoride) (PVDF) in weight ratio of 85:10:5 respectively which were dispersed in Nmethyl-2-pyrrolidone (NMP) as a solvent. The obtained slurry was then casted onto aluminum foil, and then dried at 120 ºC in a vacuum drying oven for 12 hours. Electrode disks were punched and the coin cells

were assembled in an argon-filled glove box and tested by galvanostatic charge-discharge cycling between 2.5 and 4.3 V (versus Li^+/Li) using (Kimia stat-5 V/10 mA, kimia pardaz rayane, Iran) battery tester. The cyclic voltammetry (CV) between 2.5-4.5 V (*vs.* Li^+/Li), with scan rate 0.5 mV/s and electrochemical impedance spectra (EIS) test in the frequency range of 0.01–100,000 Hz was performed on a Galvanostat/Potentiostat Autolab (PGSTAT 302N). All electrochemical measurements were carried out at room temperature.

3. RESULTS AND DISCUSSION

Fig. 1 shows the XRD patterns of the LFP powder, LFP/C_{ex}, and LFP/C_{in} composite. All diffraction peaks agree well with those of olivine LFP indexed with orthorhombic Pnma space group (JCPDS Card No. 40-1499) [26]. Clearly both the LFP and LFP/C are phase pure without x-ray identifiable traces of secondary phases. On the other hand, there is no additional diffraction peaks with crystal modification by carbon, which means the carbon is produced from glucose is amorphous. Fig. 1 (red line) show the XRD pattern of the in-situ carbon-coated sample LFP in glucose solution, the strong and sharp LFP/C_{in} peaks suggest that in-situ carbon source during synthesis has a synergism with solvent. This synergetic effect of glucose with the glycerol as a co-solvent in hydrothermal process has an undeniable role on the physical structure and electrochemical properties of nano-composite. It can clearly show that LFP/C_{in} particles have a good crystallization and well and narrow size distribution [27].

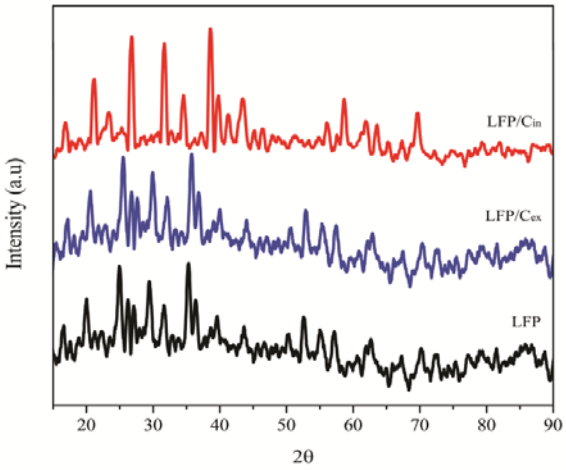

Fig. 1. XRD pattern of the as-prepared $LiFePO_4$, $LiFePO_4/C_{ex}$, $LiFePO_4/C_{in}$ powders

Fig. 2 shows the SEM images of the LFP/C_{in} sample, Fig. 2(a), and the LFP/C_{ex} sample, Fig. 2(b). The particle size of LFP/C_{in} and $LiFePO_4/C_{ex}$ is approximately 65 and 100 nm, respectively indicating that the in-situ carbon source plays a major role in determining the morphology and size distribution of particles and their growth of LFP during the

hydrothermal synthesis process. The uniformed size distribution of the particles and its porosity can essentially effect on the interface reaction between the electrode and the electrolyte solution, which means that the diffusion rate of lithium ions insertion/extraction. The glucose not only cane efficiently impact on the size of particles but also has an undeniable role on the morphology. According to the Fig. 2 (b) it is clearly revealed that the in-situ carbon sources can efficiently effect on the obtained samples' structures. Glucose as a carbon source and glycerol as a co-solvent, can change effectively the viscosity of hydrothermal media, in addition they has an essential impact on the crystal growth of obtained samples.

The TEM images Fig. 2 (d) shows that LFP/C_{ex} aggregate of several smaller particles which agglomerate around large particles. Clearly, because of the high interfacial energy, LFP/C_{ex} nanocomposites tend to assemble irregularly, which can significantly affect their specific surface area. The TEM image in Fig.2 (d) demonstrates Rhombus particles with wide particle size distribution (100-300 nm) that contain an ununiformed carbon layer. This inhomogeneous carbon coating on the LFP/C_{ex} sample may have effect on the lithium diffusion as a result it can lead to an inadequate electronically conduction [28].

According to the Fig. 2 (c) the agglomeration of particles is tremendously reduced for LFP/C_{in}.

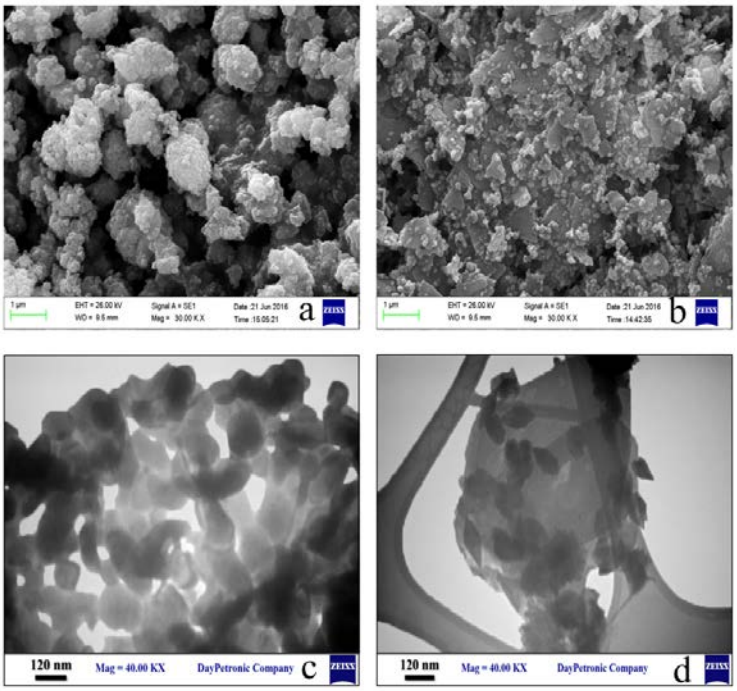

Fig. 2. SEM images of LFP/C_{in} (a); LFP/C_{ex} (b) and TEM images of LFP/C_{in} (c); LFP/C_{ex} (d)

In addition, the average particle size 50 nm approximately, illustrate a uniform pore and particle size distribution in comparison with other samples. As shown in Fig. 2 (c) monitors

that LFP/C_{in} particles encompassed in a continuous amorphous and conductive carbon shell. This continues network of carbon can explain its better electrical conductivity rather than other samples. This result demonstrated that in-situ carbon coating layer can effectively prevent the agglomeration of sample particles and make them more uniformly.

Fig. 3 shows the initial charge–discharge curves of the LFP, LFP/C_{ex} and LFP/C_{in} samples (a) and discharge capacity *vs.* cycle number for investigation of cycling performance of the three composite electrode (b). As shown in Fig. 3(a), the initial discharge capacity of LFP/C_{in}, LFP/C_{ex} and LFP deliver 133.92 mAh g^{-1}, 126.65 mAh g^{-1}, 115.52 mAh g^{-1} respectively at a constant charge/discharge current rate of 0.1 C between 2.3 V and 4.6 V(*vs* Li/Li^+). The voltage difference between the charge and discharge plateaus (ΔV) in Fig. 3(a) indicates the polarization degree of the cell system, which the LFP/C_{in} has the lowest difference potential among samples. The smaller polarization degree (smaller ΔV), can obtained the better electrochemical performance due to lower overpotentials for redox reaction for both charge-discharge processes [29].

As shown in Fig. 3b, the LFP/C_{in} nano composite delivers a discharge capacity about 129 mAh g^{-1} after 40 cycles nearly 96.3% retention capacity. The LFP electrode without carbon coating exhibits poor cycling stability and rapid and continuous fading of the discharge capacity to 70 mAh g^{-1} after 40 cycles. Both the initial discharge capacity and good cycling stability can be attributed to the unique morphologies cauliflower-like structure and ultrafine particles which can shortening the transmission length of Li^+ ions and provide the conducting pathway for the Li^+ ions into the cathode.

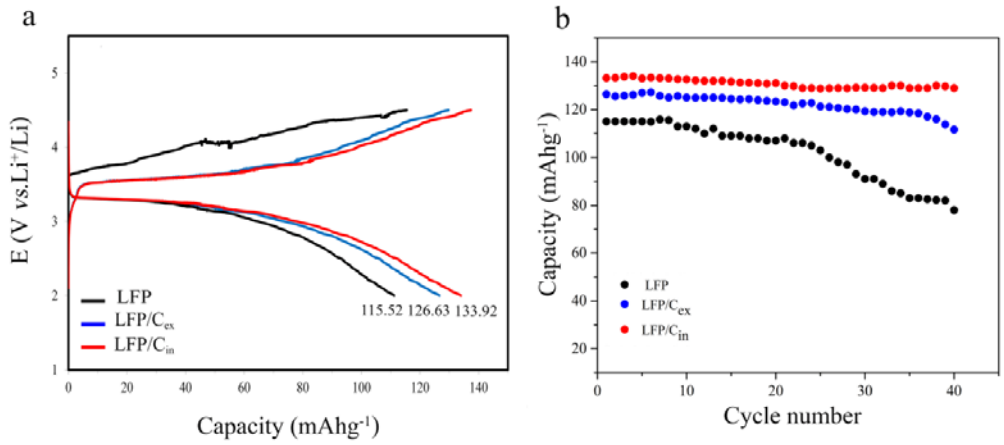

Fig. 3. (a) Initial charge-discharge profiles at 0.1 C current rates; (b) Cycling performance LFP, LFP/C_{ex} and LFP/C_{in} by the Li foil as reference and counter electrode and between 2.5-4.2 V (*vs.* Li/Li^+)

In order to investigate the effect of carbon on electrochemical performance, cyclic voltammetry (CV) and electrochemical impedance spectroscopy (EIS) measurement was used. Fig. 4 shows the CV curves of the as-synthesized $LiFePO_4$ base and Li foil electrodes at

the scan rate 0.5 $mV.s^{-1}$ and between 2.5−4.3 V (*vs.* Li/Li^+). Two samples exhibit a pair of redox peaks around 3.45 V (*vs.* Li^+/Li), correspond to Fe^{2+}/Fe^{+3} transformation during charge/discharge plateaus shown in Fig. 3(a). The results of the Fig. 4 are given below in Table 1. As can be seen in Fig. 4 the LFP/C_{in} electrodes has sharp and highly symmetrical current peaks than the LFP/C_{ex} electrode, indicating rapid electrochemical kinetics process of the cathode materials (Li^+ insertion/de-insertion). Difference between the potential of reduction and oxidation peaks of LFP/C_{in} is about 0.78 V. LFP/C_{in} demonstrates the low potential separation between the cathodic and anodic peaks (ΔEp), indicating less polarization and electrode reaction reversibility [30]. This result suggests that the LFP/C_{in} electrode has low polarization and good electronic conductivity, which means modifying electrochemical properties.

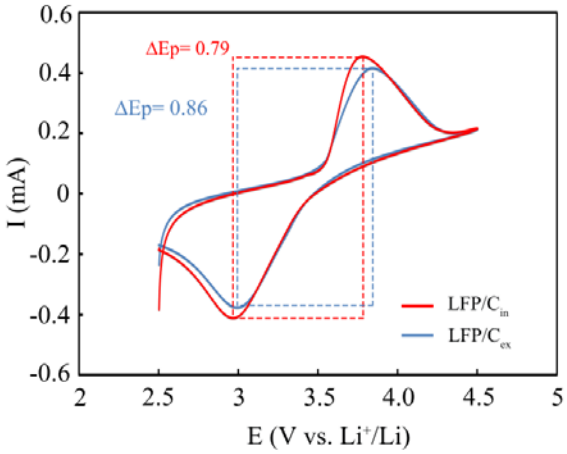

Fig. 4. Cyclic voltammograms (CVs) of LFP/C_{in} and LFP/C_{ex} electrode at scan rate of 0.5 $mV.s^{-1}$

Table 1. Cyclic voltammetry parameters of $LiFePO_4$ based on the Fig. 4

Sample	ΔEp (V)	I_c (A)	I_a (A)	I_c/I_a
LFP/C_{ex}	0.85	0.377	0.415	0.90
LFP/C_{in}	0.78	0.42	0.451	0.94

EIS measurements of LFP electrodes are performed at frequencies from 100 kHz to 0.01 Hz with an excitation voltage of 10 mV and the Nyquist plots are shown in Fig. 5. All EIS profiles include a semicircle in the high frequency region (R_{ct}) for lithiation reaction at the interface of electrolyte and cathode, in addition a straight line in the low frequency region which represents to Warburg (W) related to diffusion of the lithium ions in the electrolyte

into the bulk electrode material. The intercept impedance on the Z′-axis corresponds to the solution resistance, which consisted of the resistance of the electrolyte and electrode (R_s) [31]. The result of fitted impedance parameters are shown in Table 2. The initial R_s of the three electrodes is nearly the same (Table 2). From Fig. 5, it can be clearly seen that the diameter of the semicircle for LFP/C_{in} (120 Ω) electrode is smaller than LFP/C_{ex} (380 Ω) and LFP (420 Ω) electrode. This result indicating a significant decrease in charge transfer resistance of LFP/C_{in} material and exhibits a good correlation with capacity results in Fig. 3, due to the unique multiple conductive networks and increasing in electrical conductivity.

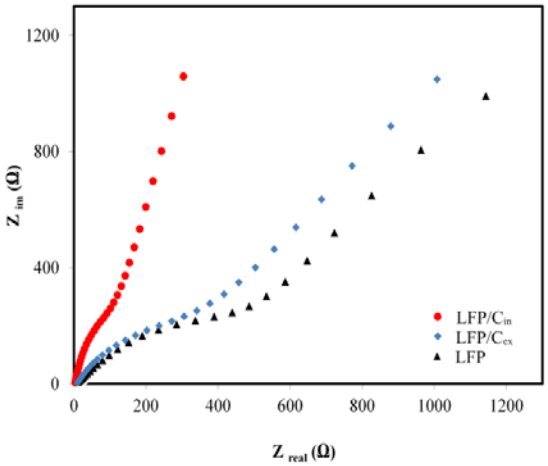

Fig. 5. EIS profiles of LFP/C_{in}, LFP/C_{ex} and LFP electrode

Table 2. Impedance parameters of LFP electrodes based on the Fig. 5

sample	R_s (Ω)	R_{ct} (Ω)	C_{dl} (μF)
LFP	11.03	420	53
LFP/C_{ex}	9.42	380	90
LFP/C_{in}	9.16	120	104

LFP/C_{in} shows higher lithium ion diffusion coefficient with increase the slope of Warburg line than the LFP/C_{ex} and LFP composite, demonstrated that the carbon coating enhanced mobility of lithium ions in LFP electrode [31,32]. All results are in good agreement with the electrochemical cycling performance of the LFP/C_{in} cathode, TEM and SEM observation.

4. CONCLUSIONS

In this work, we synthesized of LFP cauliflower-like (nanocomposite) by a hydrothermal method. The morphology and properties of cathode materials have been characterized by

XRD, SEM, TEM analysis, which confirmed the uniform olivine structure indexed by orthorhombic Pnma and size of particles about 65 nm for LFP/C_{in} and good distribution of carbon in the structure during the reaction. The CV and EIS results indicated that 10% glucose content can improve the kinetics of lithium insertion/de-insertion in the electrode material, reversible behavior and the R_{ct} is reduced as follows, LFP> LFP/C_{ex}> LFP/C_{in}. The LFP/C_{in} exhibited an initial discharge capacity (133.92 mAh g^{-1}) with the capacity retention rate of 96.3% at 0.1 C. Due to its good electrochemical performance, the LFP/C_{in} cauliflower-like can be considered as a promising cathode material for lithium-ion batteries.

Acknowledgement

The authors gratefully acknowledge the Renewable Energy Research Center (Amirkabir University of Technology, Tehran, Iran) for financial and technical support of this work.

REFERENCES

[1] J. B. Goodenough, and K. S. Park, J. Am. Chem. Soc. 135 (2013) 1167.
[2] B. Scrosati, and J. Garche, J. Power Sources 195 (2010) 2419.
[3] R. Wagner, N. Preschitschek, S. Passerini, J Leker, and M. Winter, J. Appl. Electrochem. 43 (2013) 481.
[4] A. K. Padhi, K. S. Nanjundaswamy, and J. B. Goodenough, J. Electrochem. Soc. 144 (1997) 1188.
[5] H. C. Shin, W. I. Cho, and H. Jang, J. Electrochim. Acta 52 (2006) 1472.
[6] Y. Zhang, Q. Huo, P. Du, L. Wang, A. Zhang, Y. Song, Y. Lv, and G. Li, Syn. Metals 162 (2012) 1315.
[7] X. Lou, and Y. Zhang, J. Mater. Chem. 21 (2011) 4156.
[8] J. Wang, and X. Sun, J. Energ. Environ. Sci. 5 (2012) 5163.
[9] Y. Xie, F. Song, C. Xia, and H. Du, J. Chem. 39 (2015) 604.
[10] Z. Ma, Y. Fan, G. Shao, G. Wang, J. Song, and T. Liu, J. ACS Appl. Mater. Interfaces 7 (2015) 2937.
[11] D. Xu, X. Chu, Y. He, Z. Ding, B. Li, W. Han, H. Du, and F. Kang, J. Electrochim. Acta 152 (2015) 398.
[12] A. Fang Liu, Z. Hua Hu, Z. Biao Wen, L. Lei, and J. An, Ionics 16 (2010) 311.
[13] L. Wang, G. Liang, X. Ou, X. Zhi, J. Zhang, and J. Cui, J. Power Sources 189 (2009) 423.
[14] Z. Feng, L. Wang, Y. Wang, J. Chen, Z. He, D. Ji, and Y. Xuan Zhang, J. Alloy. Comp. 651 (2015) 712.
[15] B. Z. Lu, H. Cheng, M. Lo, and C. Y. Chung, J. Adv. Funct. Mater. 17 (2007) 3885.

[16] N. Zhou, Y. Liu, J. Li, E. Uchaker, S. Liu, K. Huang, and G. Cao, J. Power Sources 213 (2012) 100.
[17] M. Konarova, and I. Taniguchi, J. Power Sources 195 (2010) 3661.
[18] Q. Wang, S. Deng, H. Wang, M. Xie, J. Liu, and H. Yan, J. Alloy. Comp. 553 (2013) 69.
[19] B. Pei, H. Yao, W. Zhang, and Z. Yang, J. Power Sources 220 (2012) 317.
[20] J. Gao, J. Li, X. He, C. Jiang, and C. Wan, J. Electrochem. Sci. 6 (2011) 2818.
[21] M. Rastgoo-Deylami, M. Javanbakh, M. Ghaemi, H. Omidvar, and H. Ghafarian, Anal. Bioanal. Electrochem. 5 (2013) 506.
[22] M. Rastgoo-Deylami, M. Javanbakh, M. Ghaemi, L. Naji, H. Omidvar, and M. R. Ganjali, J. Electrochem. Sci. 9 (2014) 3199.
[23] F. Fathollahi, M. Javanbakh, H. Omidvar, and M. Ghaemi, J. Alloy. Comp. 627 (2015) 146.
[24] H. Ghafarian-Zahmatkesh, M. Javanbakht, and M. Ghaemi, J. Power Sources 284 (2015) 339.
[25] F. Fathollahi, M. Javanbakh, H. Omidvar, and M. Ghaemi, J. Alloy. Comp. 643 (2015) 40.
[26] V. Drozd, G. Q. Liua, R. S. Liu, H. T. Kuo, C. H. Shen, D. S. Shy, and X. K. Xing, J. Alloy. Comp. 487 (2009) 58.
[27] C. Su, X. Bu, L. Xu, J. Liu, and C. Zhang, Electrochim. Acta 64 (2012) 190.
[28] T. Azib, S. Ammara, S. Nowak, S. Lau-Truing, H. Groult, K. Zaghib, A. Mauger, and C. M. Julien, J. Power Sources 217 (2012) 220.
[29] H. Deng, S. Jin, L. Zhan, Y. anli Wang, W. Qiao, and L. Ling, J. Power Sources 220 (2012) 342.
[30] C. Y. Wu, G. S. Cao, H. M. Yu, J. Xie, and X. B. Zhao, J. Phys. Chem. 115 (2011) 23090.
[31] Z. Ma, Y. Peng, G. Wang, Y. Fan, J. Song, T. Liu, X. Qin, and G. Shao, Electrochim. Acta 156 (2015) 77.
[32] J. Lang, X. Yan, and Q. Xue, J. Power Sources 196 (2011) 7841.